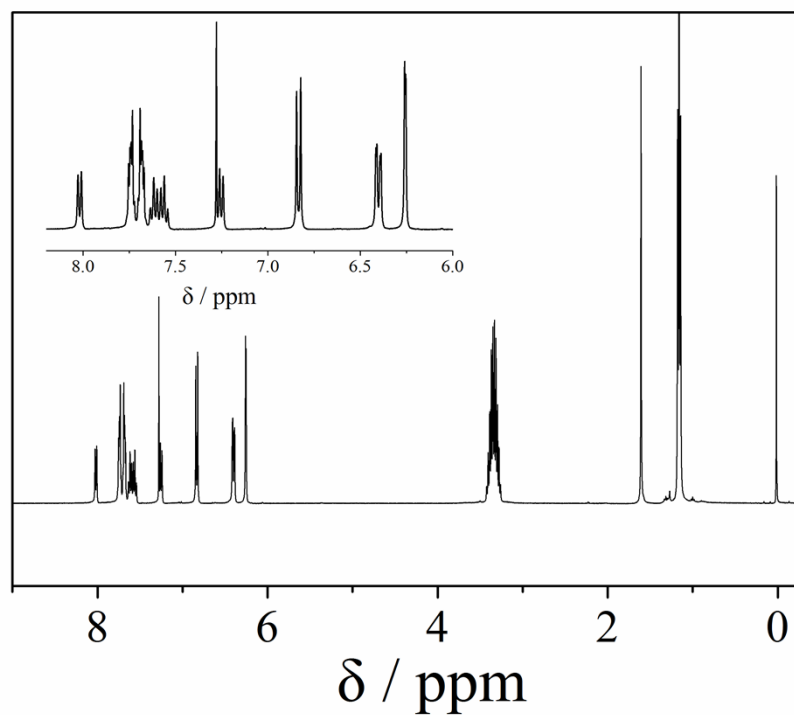


Supplementary information

**Cascade OFF-ON-OFF Fluorescent Probe: Dual Detection of  
Trivalent Ions and Phosphate Ions †**

Xuejuan Wan,<sup>a,b, §, \*</sup> Tianqi Liu,<sup>a, §</sup> Haiyang Liu,<sup>b</sup> Liqiang Gu,<sup>b</sup> and Youwei Yao<sup>b, \*\*</sup>



**Figure S1.** <sup>1</sup>H NMR spectrum of probe L.

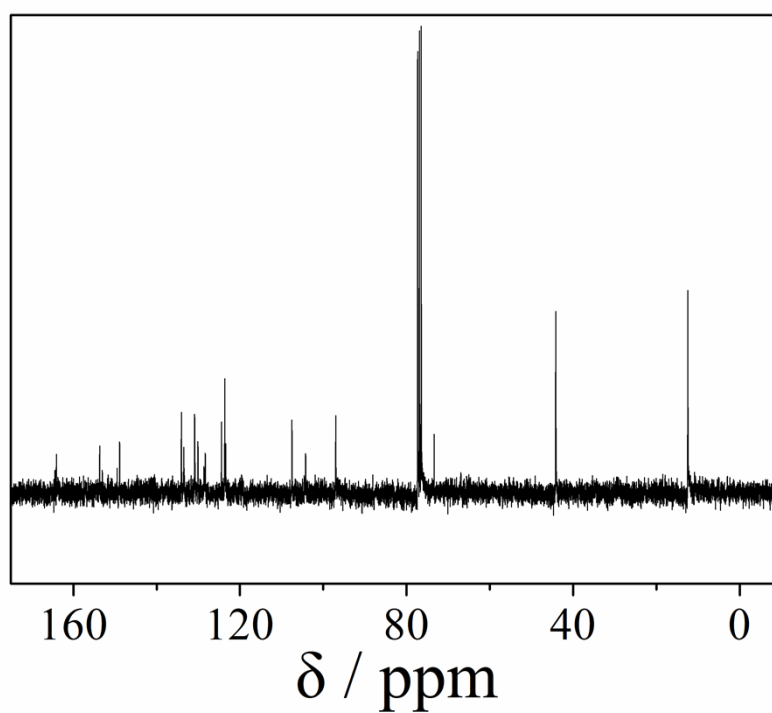


**Figure S2.** <sup>13</sup>C NMR spectrum of probe L.

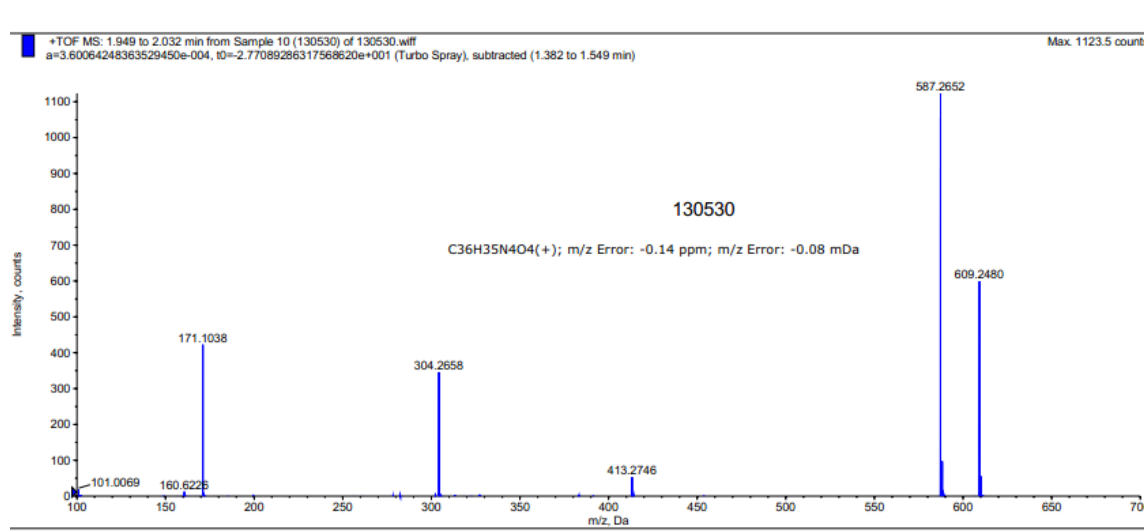


**Figure S3.** High-resolution mass spectrum of probe L.

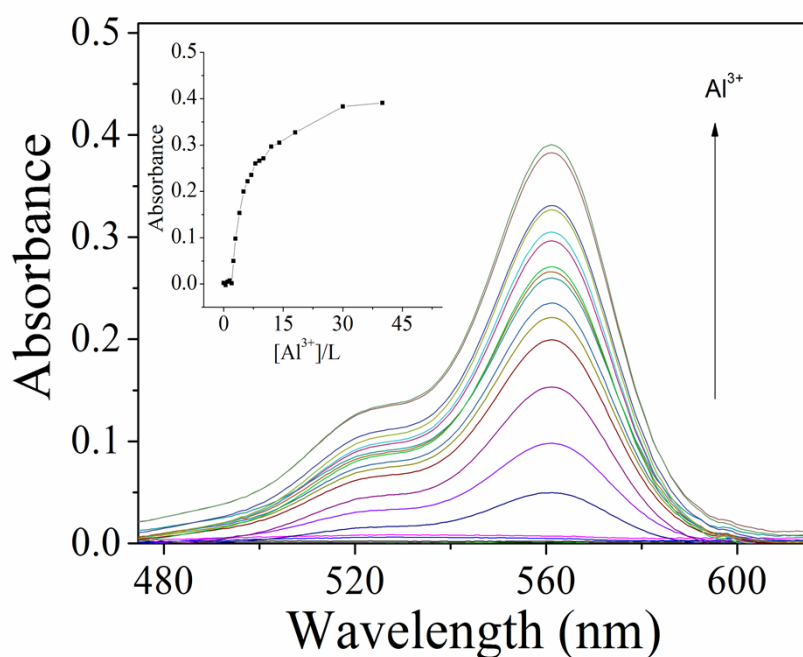


**Figure S4.** UV-vis absorption spectra obtained for probe L (25 μM) in CH<sub>3</sub>CN/Tris-buffer (1/1, v/v, pH = 7.0) with various amounts of Al<sup>3+</sup> ion. Inset: Absorbance at 564 nm of L as a function of [Al<sup>3+</sup>].

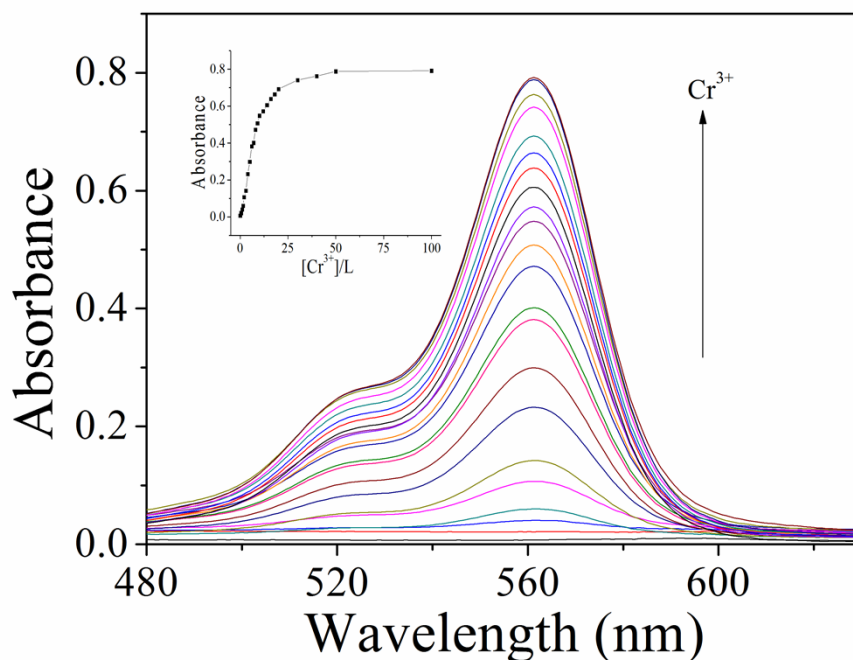


**Figure S5.** UV-vis absorption spectra obtained for probe L (25 μM) in CH<sub>3</sub>CN/Tris-buffer (1/1, v/v, pH = 7.0) with various amounts of Cr<sup>3+</sup> ion. Inset: Absorbance at 564 nm of L as a function of [Cr<sup>3+</sup>].

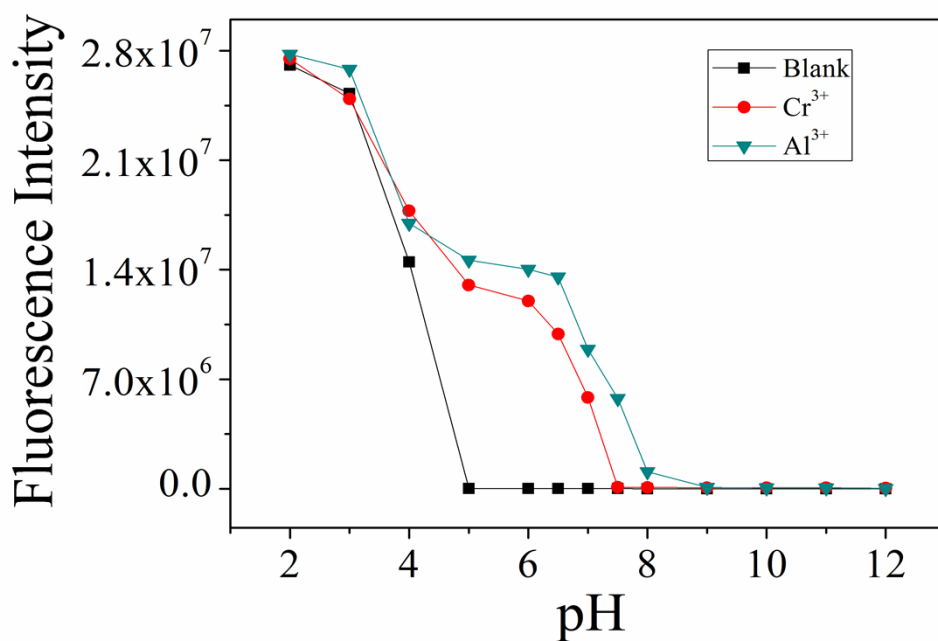


**Figure S6.** Fluorescence spectra of L (10  $\mu\text{M}$ ) in the absence and presence of  $\text{Al}^{3+}$  or  $\text{Cr}^{3+}$  ion (80  $\mu\text{M}$  each) in  $\text{CH}_3\text{CN}/\text{H}_2\text{O}$  (1/1, v/v, pH = 7.0) at various pH values,  $\lambda_{\text{ex}} = 520 \text{ nm}$ .

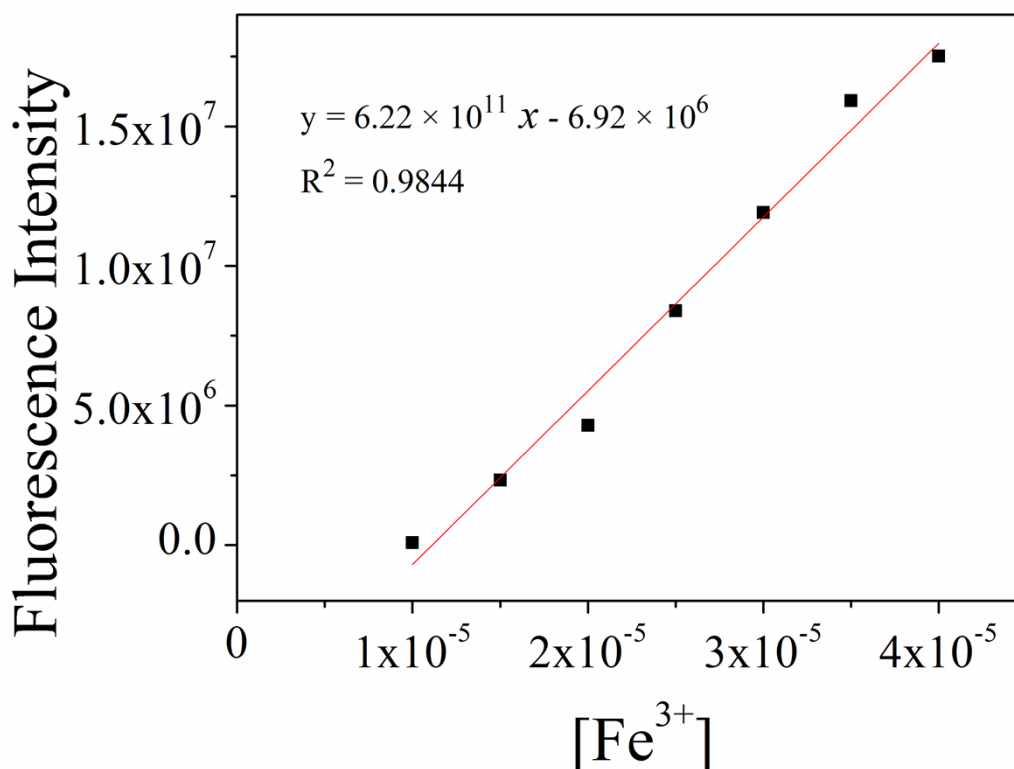


**Figure S7.** Linear response of fluorescence intensity at 586 nm of L (10  $\mu\text{M}$ ) to the  $\text{Fe}^{3+}$  concentrations changes in  $\text{CH}_3\text{CN}/\text{Tris}$ -buffer (1/1, v/v, pH = 7.0). The unit of  $x$  is mol/L.

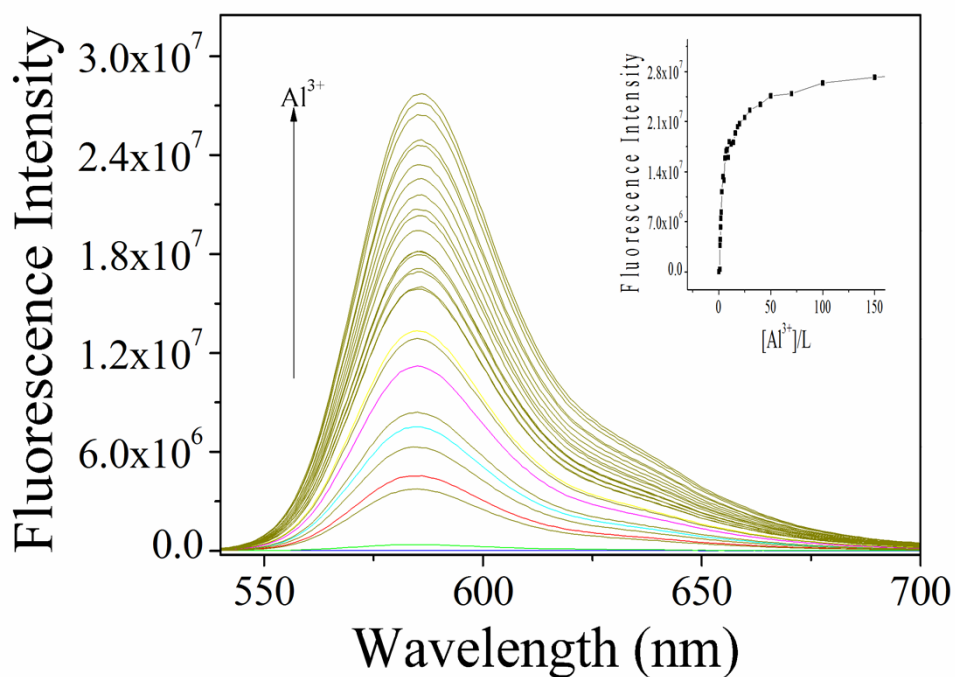


**Figure S8.** Fluorescence titrations of L (10  $\mu\text{M}$ ) with  $\text{Al}^{3+}$  ion in  $\text{CH}_3\text{CN}/\text{Tris}$ -buffer (1/1, v/v, pH = 7.0). Inset: Change of fluorescence emission intensity with the increasing amount of  $\text{Al}^{3+}$  at 586 nm,  $\lambda_{\text{ex}} = 520$  nm.

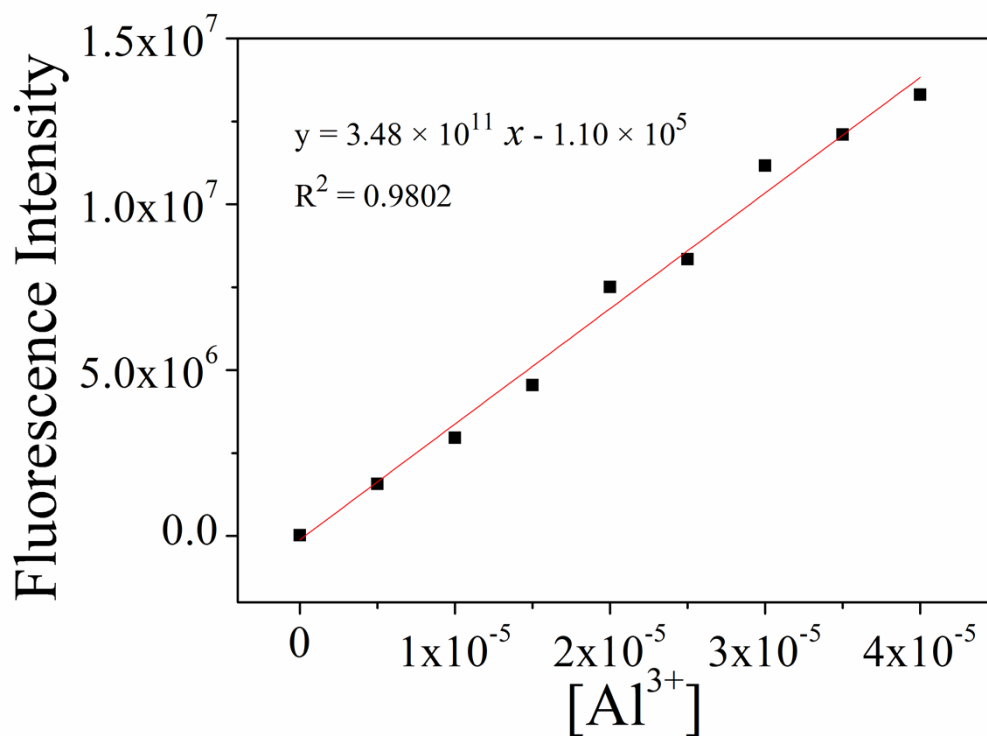


**Figure S9.** Linear response of fluorescence intensity for L (10  $\mu\text{M}$ ) at 586 nm to the  $\text{Al}^{3+}$  concentration changes in  $\text{CH}_3\text{CN}/\text{Tris}$ -buffer (1/1, v/v, pH = 7.0). The unit of  $x$  is mol/L.

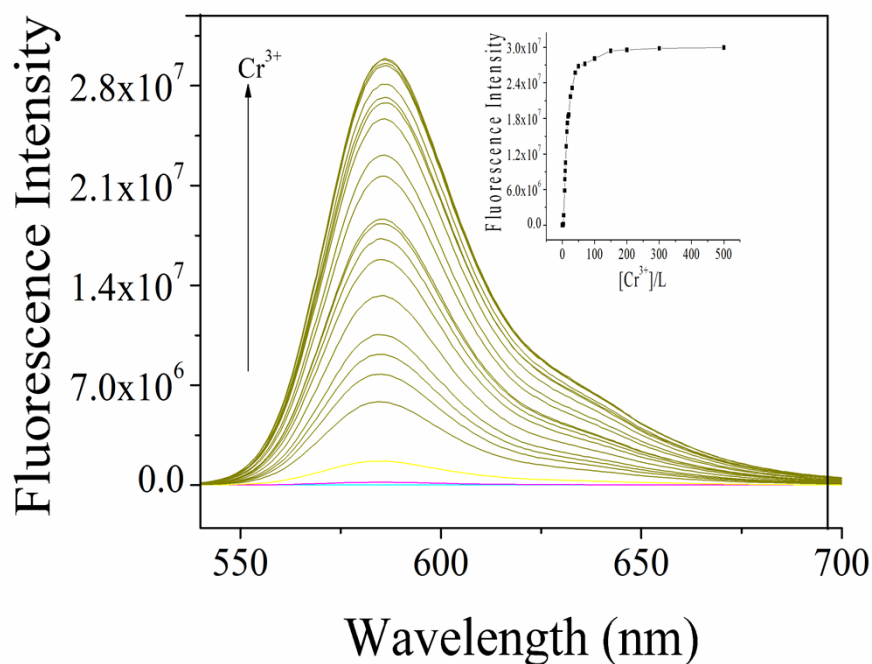


**Figure S10.** Fluorescence titrations of L (10 μM) with Cr<sup>3+</sup> ion in CH<sub>3</sub>CN/Tris-buffer (1/1, v/v, pH = 7.0). Inset: Change of fluorescence emission intensity with the increasing amount of Cr<sup>3+</sup> at 586 nm, λ<sub>ex</sub>= 520 nm.

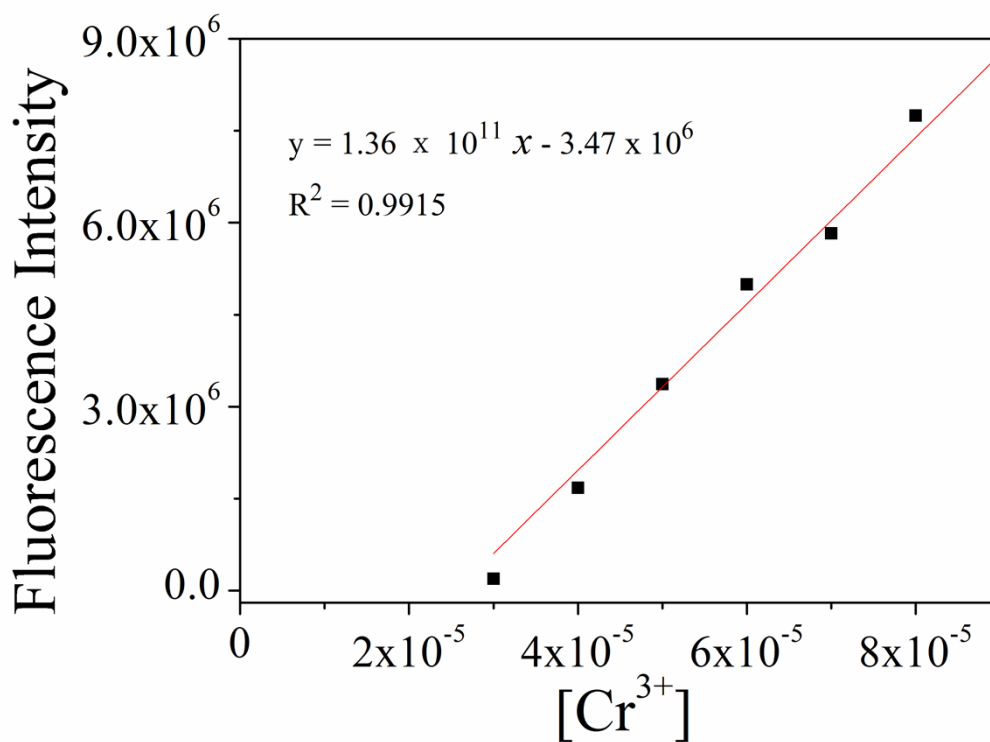


**Figure S11.** Linear response of fluorescence intensity for L (10 μM) at 586 nm to the Cr<sup>3+</sup> concentration changes in CH<sub>3</sub>CN/Tris-buffer (1/1, v/v, pH = 7.0). The unit of  $x$  is mol / L.

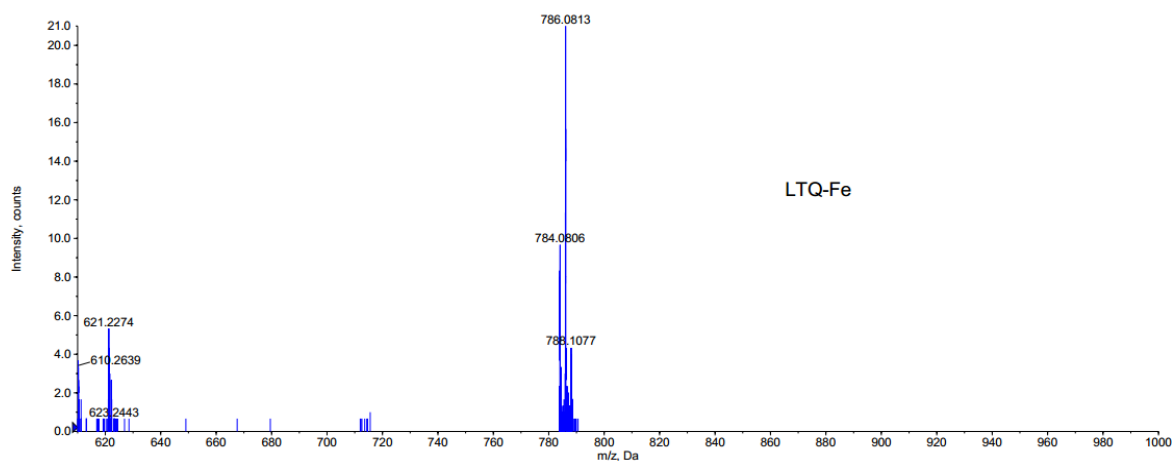


**Figure S12.** High-resolution mass spectrum of L-Fe<sup>3+</sup> complex.

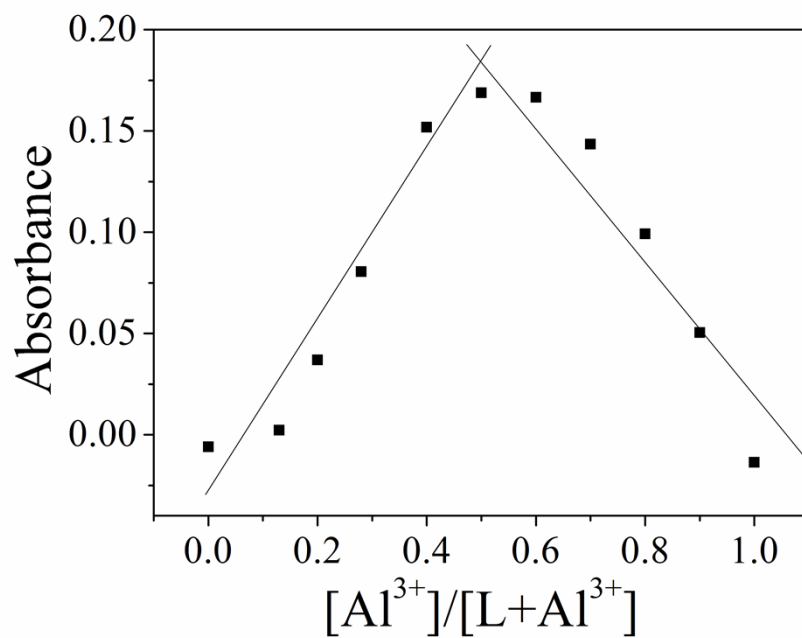


**Figure S13.** Job's plot for the determination of binding stoichiometry between L and Al<sup>3+</sup> ion in CH<sub>3</sub>CN/Tris-buffer (1/1, v/v, pH = 7.0).

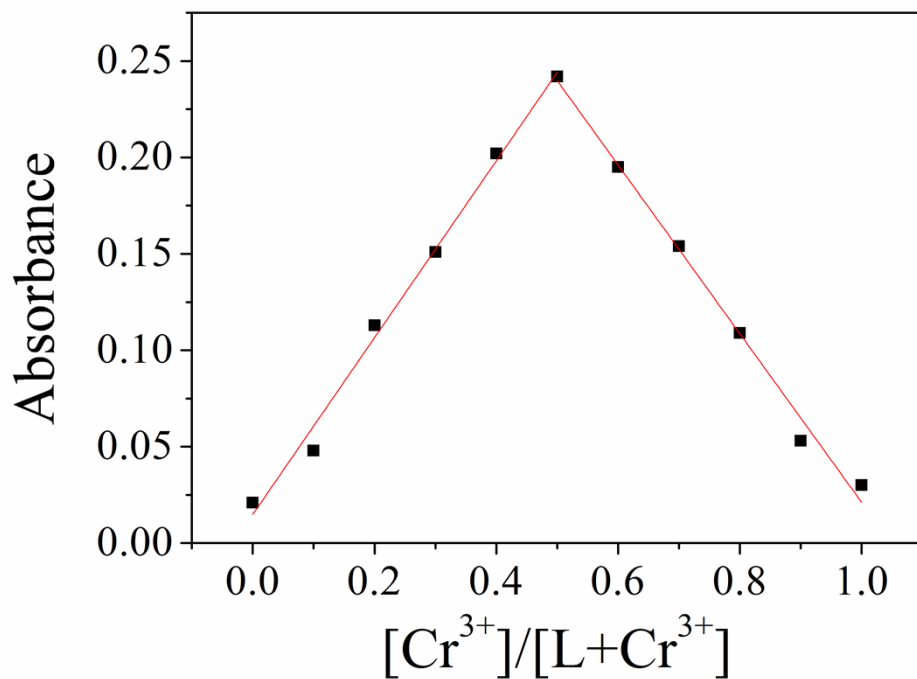


**Figure S14.** Job's plot for the determination of binding stoichiometry between L and Cr<sup>3+</sup> ion in CH<sub>3</sub>CN/Tris-buffer (1/1, v/v, pH = 7.0).

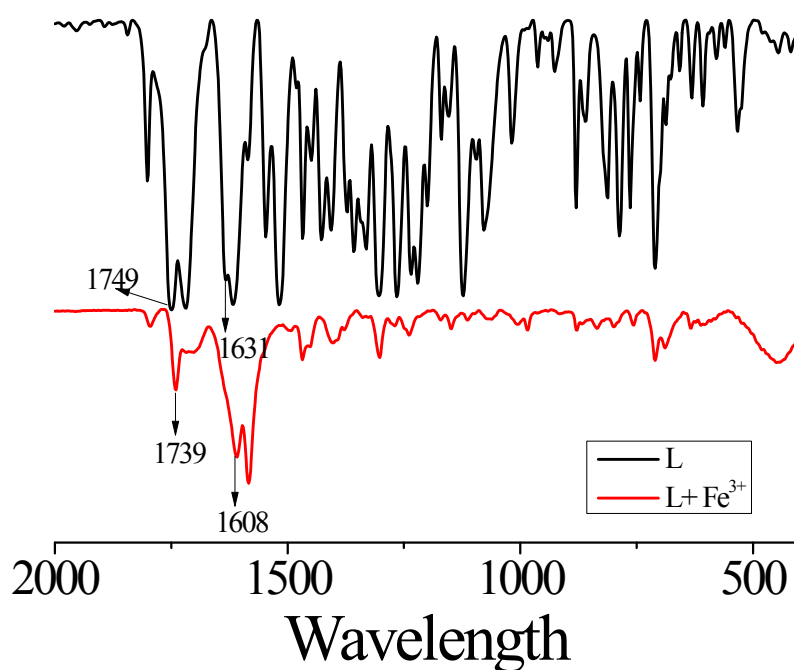


**Figure S15.** FT-IR spectra of probe L and L-Fe<sup>3+</sup> complex



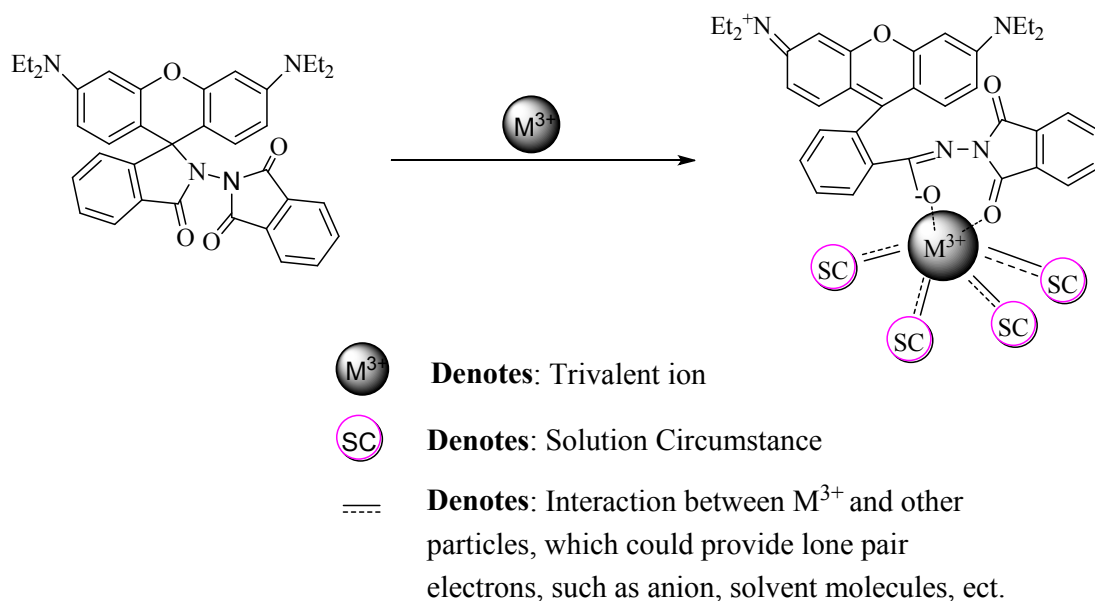
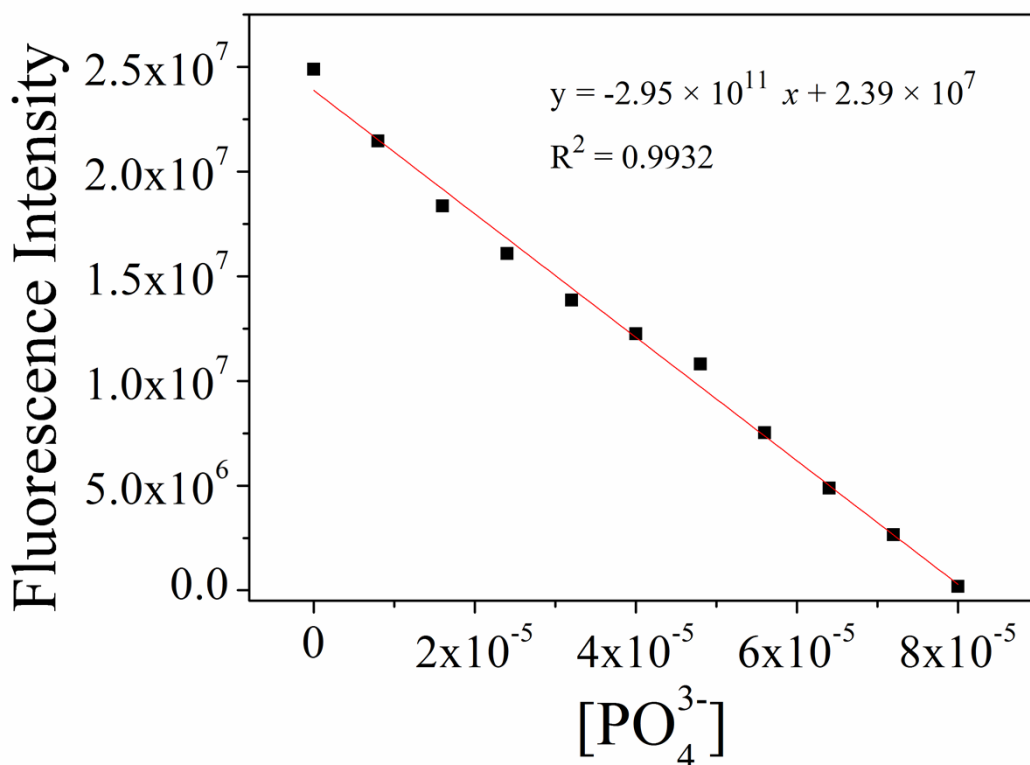
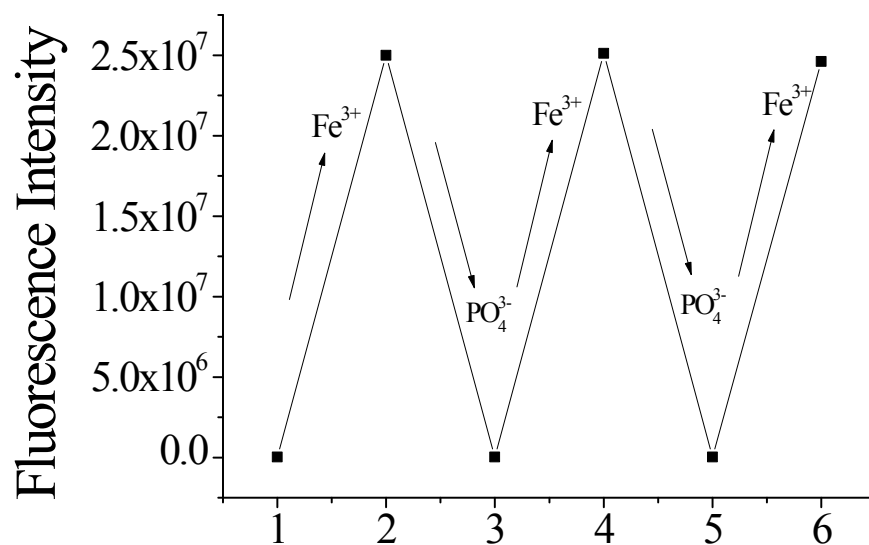


Figure S16. Proposed mechanism for the recognition of trivalent ion



**Figure S17.** Linear response of fluorescence intensity at 586 nm of the L-Fe<sup>3+</sup> complex to the PO<sub>4</sub><sup>3-</sup> concentration changes in CH<sub>3</sub>CN/Tris-buffer (1/1, v/v, pH = 7.0), [L] = 10 μM, [Fe<sup>3+</sup>] = 80 μM. The unit of  $x$  is mol/L.



**Figure S18.** Cascade fluorescence OFF-ON-OFF response of probe L with alternate addition of Fe<sup>3+</sup> cation and PO<sub>4</sub><sup>3-</sup> anion.

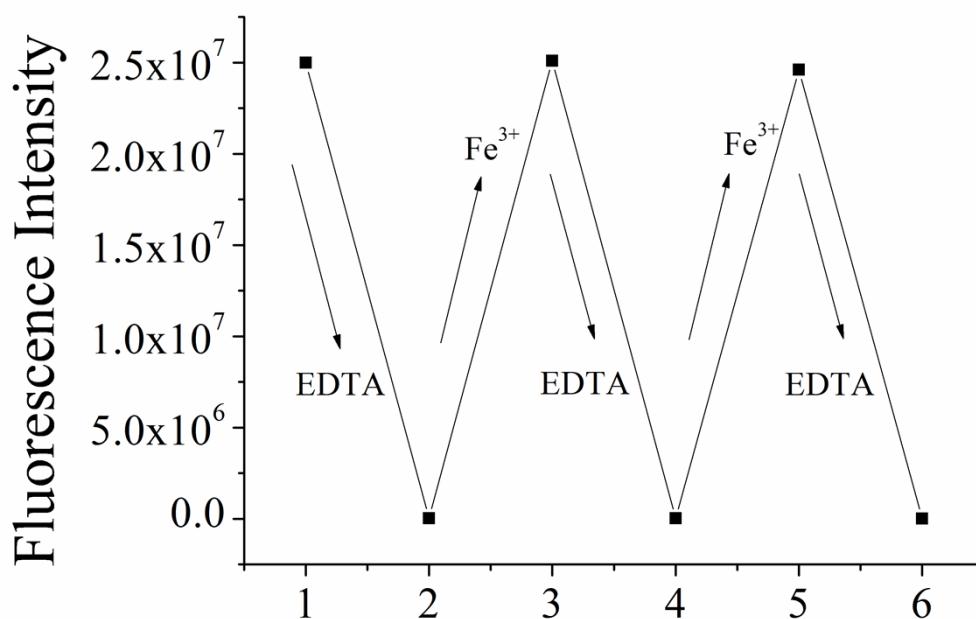


**Figure S19.** Reversibility of the Fe<sup>3+</sup> sensing process against the addition of chelating agent EDTA.